Published in final edited form as:

Leukemia. 2016 November ; 30(11): 2187–2197. doi:10.1038/leu.2016.96.

A Novel Hypoxia-Selective Epigenetic Agent RRx-001 Triggers Apoptosis and Overcomes Drug Resistance in Multiple Myeloma Cells

Deepika Sharma Das[1], **Arghya Ray**[1], **Abhishek Das**[2], **Yan Song**[1], **Bryan Oronsky**[3], **Paul Richardson**[1], **Jan Scicinski**[3], **Dharminder Chauhan**[1,¶,*], and **Kenneth C. Anderson**[1,¶,*]

[1]LeBow Institute for Myeloma Therapeutics and Jerome Lipper Myeloma Center, Department of Medical Oncology, Dana-Farber Cancer Institute, Harvard Medical School, Boston, MA

[2]Program in Cellular and Molecular Medicine, Childrens Hospital, Boston, MA

[3]EpicentRx, Inc., Mountain View, CA

Abstract

The hypoxic bone-marrow (BM) microenvironment confers growth/survival and drug-resistance in multiple myeloma (MM) cells. Novel therapies targeting the MM cell in its hypoxic-BM milieu may overcome drug resistance. Recent studies led to the development of a novel molecule RRx-001 with hypoxia-selective epigenetic and Nitric Oxide-donating properties. Here we demonstrate that RRx-001 decreases the viability of MM cell lines and primary patient cells, as well as overcomes drug-resistance. RRx-001 inhibits MM cell growth in the presence of BM stromal cells. RRx-001 induced apoptosis is associated with: 1) activation of caspases; 2) release of ROS and nitrogen-species; 3) induction of DNA damage via ATM/γ-H2AX; and 4) decrease in DNA methytransferase (DNMT) and global methylation. RNA interference study shows a predominant role of DNMT1 in MM cell survival versus DNMT3a or DNMT3b. Deubiquitylating enzyme USP7 stimulates DNMT1 activity; and conversely, USP7-siRNA reduced DNMT1 activity and decreased MM cell viability. RRx-001 plus USP7 inhibitor P5091 triggered synergistic anti-MM activity. MM xenograft studies show that RRx-001 is well tolerated, inhibits tumor growth, and enhances survival. Combining RRx-001 with pomalidomide, bortezomib or SAHA induces synergistic anti-MM activity. Our results provide the rationale for translation of RRx-001, either alone or in combination, to clinical evaluation in MM.

¶Address correspondence: Kenneth Anderson Kenneth_Anderson@dfci.harvard.edu; and Dharminder Chauhan, Dharminder_Chauhan@dfci.harvard.edu.

*Joint Senior authors

Authors' contributions: DSD designed and performed the experiments, interpreted data, and wrote the manuscript; AD helped in acquiring confocal images, AR and YS helped with animal experiments; PR contributed clinical samples; BO and JS reviewed the manuscript; DC designed research, analyzed data, and wrote the manuscript; and KCA analyzed data and wrote the manuscript.

Conflict-of-interest disclosure BO and JS are employee of EpicentRx; KCA is on Advisory board of Celgene, Millenium, Gilead, and Sanofi Aventis, and is a Scientific founder of Oncopep and acetylon; DC is consultant to EpicentRx Inc. The remaining authors have no competing financial interest.

Supplementary information is available at leukemia's website.

Introduction

Multiple myeloma (MM) remains incurable in many cases despite novel therapies, highlighting the need for further identification of factors in the host-MM bone marrow (BM) microenvironment that mediate tumorigenesis and drug resistance[1, 2]. The hypoxic-BM microenvironment[3] confers epigenetic alterations in MM cells and promotes both angiogenesis and metastasis[4–6]. DNA methylation is a major epigenetic mechanism that: 1) modulates expression of tumor suppressor genes; 2) maintains genomic integrity; and 3) play a critical role in initiation and progression of cancers, including MM[7–9]. Recent studies show that alterations in DNA methylation induce MM cell growth and drug resistance[10]. Importantly, DNA hypermethylation of genes is associated with the progression of monoclonal gammopathy of unknown significance (MGUS) to MM and from MM to plasma cell leukemia[4, 11, 12]. Consistent with these findings, hypermethylation of many genes (e.g. *CDKN2A, CDKN2B, p16, p53, SOCS, RASD1, BNIP3, SPARC, DAPK, CDH-1, CD9, WIF, DKK3, ARF, or TGFβR2*) correlates with poor prognosis in MM[12–14]. The molecular mechanism(s) mediating aberrant DNA methylation in MM and its correlation with adverse clinical outcome is unclear. Nonetheless, these findings support therapeutic targeting of epigenetic aberrations such as DNA methylation in MM.

DNA methylation is regulated by a family of DNA methyltransferase (DNMT) enzymes DNMT1, DNMT3A, or DNMT3B[15]. Importantly, DNMTs have been targeted in therapeutic approaches: specifically, DNMT inhibitors 5-Azacytidine (AZA) and Decitabine are FDA approved for the treatment of hematological malignancies, myelodysplasia, and acute myeloid leukemia[16].

Recent research efforts have led to the discovery and development of a novel first-in-class oxidative epigenetic agent RRx-001 with a distinct mechanism of action compared to AZA or Decitabine[17–19]. RRx-001 allosterically modifies hemoglobin and under hypoxic conditions catalyzes the reduction of nitrite to bioavailable nitric oxide, which accumulates in poorly oxygenated tumors[19]. Nitric oxide rapidly combines with excess superoxide in the hypoxic tumors to trigger high levels of peroxynitrite (ONOO-), thereby causing oxidative stress (Fig 1). Thus, RRx-001 exerts redox and metabolic stress on tumors, which in turn inhibits DNMTs and global hypermethylation, as well as restores tumor suppressor gene function.

Preclinical studies of RRx-001 have demonstrated anti-tumor activity in refractory solid tumor models[16, 17]. A phase-1 clinical trial of RRx-001 in advanced solid tumors showed promising anti-tumor activity in a heavily pretreated population, without dose-limiting toxicities[20]. RRx-001 is currently under investigation in multiple Phase II clinical trials, alone or in combination, for the treatment of solid tumors (NCT02096354; NCT02489903; NCT02452970; NCT02215512). Here we examined the anti-MM activity of RRx-001 using both *in vitro* and *in vivo* preclinical models of MM.

Materials and methods

Cell culture and reagents

Human MM cell lines and PBMCs from normal healthy donors were cultured in supplemented RPMI-1640 medium. Tumor cells, BMSCs or plasmacytoid dendritic cells (pDCs) from MM patients were isolated and cultured as described previously[21]. Informed consent was obtained from all patients in accordance with the Helsinki protocol. Drug Sources: RRx-001 was obtained from EpicentRx, Inc (USA); pomalidomide, P5091, SAHA, 5-azacytidine, and bortezomib were purchased from Selleck chemicals (USA).

Cell viability, cell growth and apoptosis assays

Cell viability was assessed by WST-1/CellTiter-Glo Luminescent assays, as previously described[22,23]. DNA synthesis was measured by ^{3}H-TdR uptake. Apoptosis was measured using Apo-Direct TUNEL assay, and Annexin/PI staining[24].

Cell migration, angiogenesis assays and western blotting

24-well Transwell plates (Millipore, MA) were used to perform cell migration assays as previously described.[24] Angiogenesis was measured, as previously described.[24] Immunoblot analysis was performed using antibodies (Abs) against caspase-8, caspase-9, caspase-3, PARP, ATM, p53, ku70, γ-H2AX, HDM2, p21, DNMT1 or GAPDH (Cell Signaling, Beverly, MA) DNMT3a or DNMT3b (Bethyl Laboratories, Montgomery, TX).

Assessment of Reactive Oxygen Species (ROS), Nitric oxide (NO), Mitochondrial membrane potential (ΔΨm), Nitrosylation, and Nitrotyrosine levels

Cellular ROS and NO levels were detected using assay kits (Abcam, Cambridge MA). **ΔΨm** was measured using MitoPT™ JC-1 assay kit. Nitrosylation plus nitrotyrosine modification of proteins was analyzed using (S-NO) detection assay kit and OxiSelect Nitrotyrosine ELISA kit.

Transfection assays

MM.1S cells were transiently transfected with control scr siRNA, DNMT1 siRNA, DNMT3A siRNA, DNMT3B flexitube siRNA or USP7 siRNA using the cell line Nucleofector kit V (Amaxa Biosystems, Cologne, Germany).

DNMT activity assays

EpiQuik DNA methyltransferase activity kit was utilized to measure total DNMT activity. Global DNA methylation was assessed using MethylFlash Methylated DNA 5-mC Quantification Kit (Epigentek).

Human plasmacytoma xenograft model

All animal experiments were approved by and conformed to the relevant regulatory standards of the Institutional Animal Care and Use Committee at the Dana-Farber Cancer Institute. CB-17 SCID-mice were subcutaneously inoculated with 5.0×10^{6} MM.1S cells in 100 μL of serum-free RPMI 1640 medium, as previously described[24]. When tumors were

measurable, approximately 3 weeks after MM-cell injection, mice (5 mice/group) were randomized blindly and treated with vehicle alone, RRx-001 (5 mg/kg or 10 mg/kg, i.v.) thrice-weekly for 24 days.

Immunohistochemistry

Mice tumor sections were subjected to immunostaining for Ki67, apoptosis (TUNEL), γ-H2AX, vWF, iNOS and DNMT1 as previously described[22, 25]. Immunostained tissues were imaged by microscopy.

Statistical analysis

Statistical significance was determined by the Student's *t* test. GraphPad Prism software was used for mice survival studies. Isobologram analysis[26] was done using the CalcuSyn software program.

Results

RRx-001 inhibits MM cells growth and overcomes resistance to novel and conventional therapies

RRx-001 (1-bromoacetyl-3,3-dinitroazetidine) is a novel aerospace industry-derived agent with chemical structure and mechanism of action distinct from alkylating and epigenetic drugs (Fig 1A)[19]. To examine whether RRx-001 affects the viability of MM cells, we treated human MM-cell lines (MM.1S, RPMI-8226, H929, ARP1, KMS-11, OPM2, LR5, ANBL6.WT), along with drug resistant cell lines such as dexamethasone (MM.1R), doxorubicin (Dox40), melphalan (LR5), bortezomib (ANBL6.BR), and Hypoxia mediated apoptosis (RPMI-8226) with different concentrations of RRx-001 for 24h, followed by assessment for cell viability using WST-1 assays. RRx-001 induces a dose-dependent significant ($p < 0.05$) decrease in viability of all cell lines (Fig 1B). A significant increase in RRx-001 anti-MM activity (10%-20% increase) was noted under hypoxia versus normoxic settings (MM.1S, RPMI-8226 and DOX-40) (Supplementary Fig 1).

To determine whether RRx-001 affects viability of purified patient MM cells, purified (CD138+) MM cells were examined from 2 newly diagnosed (patients #3 and #4) and 3 refractory MM patients (Fig 1C), which were treated prior with dexamethasone (patient #1), bortezomib/dexamethasone (patients #5), and lenalidomide/bortezomib/dexamethasone (patient #2). All patient MM cells had a dose dependent decrease in cell viability with RRx-001 treatment (Fig 1C). This shows that RRx-001 can trigger cytotoxicity in bortezomib, Dex, or lenalidomide resistant patient tumor cells. In contrast, RRx-001 at the IC_{50} (1.25 μM-2.5 μM) for patient MM cells does not significantly affect normal PBMCs viability (Fig 1D). RRx-001 at high concentrations (7–10 μM) decrease PBMCs viability by 30%-70%, pointing out that normal cells are not completely refractory to RRx-001. Thus, RRx-001 possess a favorable therapeutic index in MM.

RRx-001 blocks migration of MM cells and associated angiogenesis

Previous studies showed that migration of MM cells and angiogenesis play an important role in the progression of MM[27, 28]. The effect of RRx-001 on these events was therefore

examined using transwell insert systems and *in vitro* tubule formation assays, respectively. Serum alone (control) increased MM.1S cell migration; importantly, RRx-001 inhibited serum-dependent MM.1S cell migration, as reflected by reduced crystal violet stained cells (Fig 2A, left and right panel). These cells were >95% viable before and after performing the migration assay. These data suggest that RRx-001 may negatively regulate homing of MM cells to BM, as well as egress into the peripheral blood.

To determine whether RRx-001 has anti-angiogenic activity, we used *in vitro* capillary-like tube structure formation assays. Specifically, human vascular endothelial cells (HUVECs) plated onto matrigel differentiate and form capillary-like tube structures reflecting *in vivo* neovascularization. Treatment of HUVECs with RRx-001 decreased tubule formation significantly (Fig 2B). These findings suggest that the RRx-001 blocks angiogenesis.

RRx-001 inhibits bone marrow stromal cells (BMSCs)- or plasmacytoid dendritic cells (pDCs)-induced growth of MM cells

BMSCs mediate paracrine growth of MM cells and protects against cytotoxicity of anti-MM agents by cytokine secretion[29, 30]. Treatment of BMSCs (patient 1–3) for 24h with RRx-001 (5 μM) does not decrease viability of these cells (Supplementary Fig 2). RRx-001 significantly inhibited BMSCs-induced MM.1S cell growth (Fig 2C).

Our recent studies have shown the important role of pDCs in MM pathogenesis and drug resistance[21, 31, 32]. We therefore next examined the effect of RRx-001 on pDC-induced MM growth. MM.1S cells and patient pDCs were cultured either alone or together, with or without RRx-001. RRx-001 inhibited pDCs-induced MM.1S cell growth significantly (Fig 2D). This suggests that RRx-001 not only target MM cells directly, but also overcomes the cytoprotective effects mediated by the MM-host BM microenvironment.

Mechanism(s) mediating the anti-MM activity of RRx-001

MM.1S and ANBL.6BR cells were treated with RRx-001 for 12h, and then subjected to cell cycle analysis. RRx-001 induced significant G1 phase growth arrest, with concomitant decrease in S phase in both cell lines (Fig 3A). RRx-001 triggered significant apoptosis in MM cells (Fig 3B and Fig 3C, respectively). RRx-001 triggered a marked increase in PARP and caspase-3 cleavage, a signature event during apoptosis[33](Fig 3D). Furthermore, we found that RRx-001 induced activation of both caspase-8 (extrinsic) and caspase-9 (intrinsic)-mediated apoptotic signaling cascades (Fig 3D).

RRx-001 decreases mitochondrial membrane potential (ΔΨm), as well as increases reactive oxygen and nitrogen species (RONS) in MM cells

Stress-induced apoptosis is associated with alterations in **ΔΨm** and release of ROS. The role of ROS, in particular Superoxide radical (O_2^-), in mediating apoptosis is well established[34]. As reported earlier, RRx-001 triggers oxidative (ROS/superoxide) and nitrative stress (Nitric oxide/RNS) or together termed RONS (Fig 1A).[19, 35, 36] Treatment of MM.1S cells with RRx-001 significantly decreased **ΔΨm**, with a concomitant increase in both ROS and nitric oxide levels (Fig 4A–Fig 4C, respectively). Furthermore, even short-term (2h) treatment of MM.1S cells with RRx-001 triggered a robust increase in ROS, O_2- and nitric oxide, as

evident from immunofluorescence staining assays (Fig 4D). Similar to our observations in MM.1S cells, RRx-001 increases superoxide and NO levels in RPMI-8226 and Dox-40 cells lines, albeit to a lesser extent than observed in MM.1S cells. Moreover, RRx-001 modestly increases ROS in RPMI-8226 cells, and only low-levels of ROS were observed in Dox-40 cells (Supplementary Fig 3).

Nitric oxide regulates activity of various proteins by *S*-nitrosylation and/or tyrosine nitration, which in turn modulates transcription, DNA repair, and apoptosis.[37, 38] Dysregulation of *S*-nitrosylation is linked to tumorigenesis and drug resistance in cancers.[39] We found that RRx-001 enhances *S*-nitrosylation of proteins in MM cells (Fig 4E). Similarly, modification of proteins at 3-nitrotyrosine (NO2-Tyr) residues in RRx-001-treated MM cells confirmed nitric oxide-mediated downstream oxidative stress signaling in MM cells (Fig 4F). Together, these findings suggest that anti-MM activity of RRx-001 is mediated via induction of ROS/nitric oxide/protein modification pathways.

RRx-001 triggers DNA damage response (DDR) via γ−H2AX/ATM/p53/Ku70 signaling cascade

ROS generation is associated with induction of DNA damage signaling[40, 41]. An early event in the response of mammalian cells to DNA double-strand breaks is the phosphorylation of histone H2AX (γ-H2AX) at the sites in proximity to DNA breaks[42]. RRx-001 triggered upregulation of γ-H2AX (Fig 4G). Of note, baseline γ-H2AX levels (untreated control) were observed in MM.1S cells, reflecting ongoing DNA damage in MM cells as reported in our recent study[43]. As for γ-H2AX, DNA damage response proteins ATM and p53 showed similar kinetics of induction in RRx-001-treated cells (Fig 4G). A modest induction of DNA repair protein Ku70 was also noted in RRx-001-treated MM.1S cells (Fig 4G).

We next determined whether RRx-001-induced cytotoxicity is irreversible. For these studies, we performed drug-washout experiments. MM.1S cells were treated with RRx-001 for short interval (3h); cells were then washed to remove drugs and cultured in medium without drugs for 24h. Results showed that short-term (3h) treatment with RRx-001 triggered significant cytotoxicity in MM.1S cells (Fig 4H). These data are consistent with the ability of RRx-001 to trigger ROS/NO and DNA damage within 2h in MM cells (Fig 4D, and data not shown). Washout experiments showed that a short time exposure of MM cells to RRx-001 is sufficient to initiate ROS/NO-associated apoptotic signaling and cytotoxicity.

RRx-001 inhibits DNA methylation by downregulating DNA methytransferases (DNMTs)

Our data (Fig 4) shows that RRx-001 triggers oxidative stress, which in turn can modulate epigenetic events via DNMTs. RRx-001 significantly decreased DNMT activity (Fig 5A, bar graph). In agreement with these data, RRx-001-treated MM.1S cells showed a marked decrease in the expression of DNMT1, DNMT3A, and DNMT3B (Fig 5A, immunoblot). RRx-001 decreases global methylation levels in MM cells in a dose-dependent manner (Fig 5B).

We next asked whether DNMTs are functionally significant in MM. We performed loss-of-function studies using siRNA against DNMT1, DNMT3A, and DNMT3B. The specificity of DNMT1-siRNA, DNMT3A-siRNA or DNMT3B–siRNA was evident by a substantial

decrease in the expression of respective DNMTs (Fig 5C, western blot). Importantly, transfection of DNMT1-siRNA, but not scr-siRNA, induced a significant (50% ± 3.2%) MM cell death (Fig 5C, bar graph; $p < 0.001$). On the other hand, DNMT3B–siRNA triggered a modest (15–20%) cell death, whereas DNMT3A-siRNA-tranfected MM cells showed no significant cytotoxicity (Fig 5C, bar graph). Similar findings were observed for DNMT1-siRNA in RPMI-8226 and DOX-40 cells (Supplementary Fig 4). Together, these data that DNMT1 plays a key role in MM cell survival versus DNMT3a or DNMT3b. To corroborate these data, we utilized a biochemical inhibitor of DNMT1 procainamide.[44] In concert with our RNA interference data, treatment of MM cells with procainamide decreased MM cell viability (Fig 5D), which was associated with reduced DNMT activity (Fig 5E), and global DNA methylation levels (Fig 5F).

The finding that DNMT1 plays a key role in MM (Fig 5C, bar graph), coupled with the data that RRx-001 downregulates DNMT1, suggests a potential role of DNMT1 in RRx-001-mediated anti-MM activity. To test this hypothesis, MM.1S cells were transfected with DNMT1-siRNA or scr-siRNA, and then treated with RRx-001, followed by cell viability analysis. DNMT1-siRNA-transfected MM.1S cells showed significant cell death (50%), which was not enhanced in response to treatment with RRx-001 (Fig 5G). In contrast, DNMT3B siRNA-transfected cells showed modest (15–20%) killing, which was markedly increased (50%) upon treatment with RRx-001 (Fig 5G). DNMT3A-siRNA triggered only minimal (5%) cytoxicity, and RRx-001 treatment increased (55%) cytotoxicity (Fig 5G). Our findings that DNMT1 blockade alone triggers cytotoxicity in MM cells is consistent with the similar observations in a recent report.[45] Furthermore, our prior study demonstrated efficacy of pan-DNMT inhibitor 5-azacytidine (AZA) in MM cells[46]. A comparative cytotoxicity analysis of RRx-001 with AZA showed that RRx-001 is more potent than AZA against MM cells (Supplementary Fig 5).

We also examined whether baseline expression of DNMT1 dictate sensitivity to RRx-001. Among DNMTs, DNMT1 was highly expressed, albeit differentially in all MM cell lines. Whereas low and variable expression of DNMT3a and DNMT3b was noted in all cell lines (Supplementary Fig 6A). Immunoblot analysis of protein lysates shows a higher baseline level of DNMT1 in RPMI-8226 and Dox40 versus MM.1S cells; and importantly, treatment of these cell lines with their respective IC_{50} of RRx-001 reduces DNMT1 levels (Supplementary Fig 6B). These data demonstrate that RRx-001 retains the ability to decrease DNMT1 levels irrespective of differential baseline levels of DNMT1 levels in MM cell lines. Taken together, our data show that: 1) DNMT1-siRNA induces cytotoxicity in MM cells; and importantly, the extent of cytotoxicity induced upon DNMT1 knockdown (KD) is similar to that triggered by RRx-001; 2) DNMT1 KD does not add to the cytotoxic effects of RRx-001; and 3) RRx-001 downregulates DNMT1. These findings suggest that RRx-001-triggered apoptosis in MM cells is mediated, at least in part, via DNMT1 inhibition.

Deubiquitylating (DUB) enzyme USP7 stimulates DNMT1 activity and blockade of USP7 enhances anti-MM activity of RRx-001

Analysis of DNMT1-associated proteins using STRING protein interaction database[47] showed a direct interactive link with DUB enzyme USP7 (Fig 6A). DUBs remove the ubiquitin from proteins, thereby preventing their degradation. An earlier report showed that USP7 stabilizes DNMT1 and upregulates its enzymatic activity.[48] Our data show that RRx-001 decreases DNMT1 activity (Fig 5). Based on these observations, we asked whether RRx-001-mediated decrease in DNMT1 is due to a direct inhibitory effect of RRx-001 on USP7. No significant USP7 inhibition was observed in RRx-001-treated MM cells (data not shown). USP7-siRNA decreased DNMT1 activity in MM.1S cells (Fig 6B, bar graph). Next, we studied whether USP7 inhibition enhances activity of RRx-001 by triggering a more pronounced decrease in DNMT1 activity. Importantly, treatment of USP7-siRNA-transfected cells with RRx-001 showed a more robust cytotoxicity than triggered by either USP7-siRNA or RRx-001 alone (Fig 6C).

To further confirm our findings with USP7-siRNA, we utilized USP7 inhibitor P5091 and examined whether the combination of RRx-001 with P5091 induces additive anti-MM activity. MM.1S, ARP-1, and RPMI-8226 cells were treated with RRx-001 and P5091 across a range of concentrations. Analysis of synergistic anti-MM activity by the Chou and Talalay method[26] showed a significant decrease in viability of all cell lines with combined RRx-001 and P5091, compared to either agent alone (Fig 6D and supplementary fig 7). A combination index of < 1.0 in all MM cell lines tested confirmed the synergistic anti-MM activity. Importantly, combined RRx-001 and P5091 triggered greater DNMT1 inhibition than either agent alone (Fig 6E).

Our earlier study showed that P5091-induced cytotoxicity is primarily mediated by a decrease in USP7 substrate HDM2 and concomitant upregulation of p53 and p21.[22] Combination of RRx-001 and P5091 markedly decreased HDM2, upregulated p53 and p21 versus either agent alone (Fig 6F).

RRx-001 inhibits MM cell growth *in vivo* and prolongs survival in a xenograft mouse model

Having shown that RRx-001 induces apoptosis in MM cells *in vitro*, we next examined the *in vivo* efficacy of RRx-001 treatment using the human plasmacytoma MM.1S xenograft mouse model[22, 24, 25]. Treatment of MM.1S–tumor-bearing mice with intravenous (i.v.) injection of RRx-001 blocks MM tumor growth and enhances survival (Fig 7A and Fig 7B). RRx-001 treatment was well tolerated, suggested by no apparent weight loss (Supplementary Fig 8).

As seen in Figure 7C and 7D, tumors from RRx-001-treated mice vs. control mice showed that RRx-001: 1) increases the number of TUNEL-positive apoptotic tumor cells; 2) decreases proliferation in tumors, as assessed by Ki-67 staining; 3) reduces angiogenesis, as evidenced by decreased staining for angiogenesis-related vWF; 4) increases γ-H2AX- and iNOS-positive tumor cells; and 5) inhibits DNMT1 expression and enzymatic activity. This shows robust *in vivo* apoptotic activity of RRx-001.

Combined treatment with RRx-001 and bortezomib, pomalidomide, or HDAC inhibitor SAHA induces synergistic anti-MM activity

Since the mechanism of action of RRx-001 is distinct from anti-MM agents, we next examined whether combining RRx-001 with these agents enhances cytotoxicity via induction of multiple apoptotic signaling pathways. Isobologram analysis[26] to assess synergistic anti-MM activity showed that low concentration combinations of RRx-001 with bortezomib, pomalidomide, or HDAC inhibitor SAHA triggers synergistic activity (Supplementary Fig 9–Fig 11). A concrete evidence of toxicity reduction with combination therapy awaits clinical trials results, but the synergy observed *in vitro* may suggest for use of lower doses with decreased side effects.

Discussion

Our studies utilized MM cell lines, patient tumor cells, and xenograft models, along with biochemical and genetic models, to show the anti-MM activity of a novel epigenetic modulator RRx-001. We show that RRx-001 decreased the viability of MM cell lines and primary patient tumor cells without markedly affecting the viability of normal PBMCs. These data suggest a selective anti-MM activity and a favorable therapeutic index for RRx-001. We found anti-MM activity of RRx-001 against various MM cell lines, including those sensitive and resistant to known drug therapies, as well as harboring distinct cytogenetic background.[49, 50] The variable IC_{50} of RRx-001 against these MM cell lines may be due to various factors such as distinct genetic profile, drug resistance characteristics[30], differential sensitivity to oxidative stress or antioxidant capacity among the MM cell lines. For example, we observed a relatively higher IC_{50} of RRx-001 for Dox40 and RPMI-8226 versus MM.1S. Another possibility is that since histone deacetylases, in particular HDAC1, modulates DNMT1[51], it is likely that RRx-001 may alter HDAC1 or other similar upstream regulators of DNMTs. The expression and/or activity levels of upstream modulators of DNMTs among MM cell lines may also account for differential sensitivity to RRx-001. Nonetheless, RRx-001 triggers cytotoxicity in all MM cell lines at the concentrations that are clinically achievable.

To determine whether RRx-001 overcomes bortezomib resistance in MM cells, we utilized previously characterized[52] bortezomib-sensitive (ANBL6.WT) and -resistant (ANBL6.BR) MM cell lines. RRx-001 showed significant anti-MM activity in ANBL6.BR cells, confirming the ability of RRx-001 to overcome bortezomib-resistance. Moreover, we found consistently low IC_{50} of RRx-001 against tumor cells from patients with MM resistant to bortezomib, lenalidomide, and dexamethasone. We found that RRx-001 inhibits MM cell growth, even in the presence of BM stromal cells or other BM accessory cells including pDCs. Thus, RRx-001 overcomes drug resistance in MM. Moreover, RRx-001 treatment decreases the viability of *p53*-null ARP-1 MM cells (Fig 1B). As 10–15% of MM patients at diagnosis have drug resistance conferring p53 mutations/deletions, and these abnormalities are acquired with disease progression, a therapeutic approach using RRx-001 would possess activity even in this setting.

Mechanistic studies show that RRx-001-triggered apoptosis is associated with activation of caspases and PARP; release of Reactive oxygen and nitrogen species (RONS); induction of

DNA damage response signaling via ATM/p53/γH2AX/p21; post-translational modification of proteins via *S*-nitrosylation or tyrosine nitration and decrease in DNA methytransferase DNMT1 activity along with global methylation levels. Our finding in MM cells is consistent with similar observations using RRx-001 in other cell systems[53, 54].

Induction of ROS affects DNA methylation by directly interacting with DNA molecules and/or by altering levels of DNMTs[55]; consistent with this data, we found that RRx-001-induced ROS is associated with decreased expression of DNMT1, DNMT3A, and DNMT3B. Among DNMTs, DNMT1 is more functionally relevant in MM, since DNMT1-siRNA triggered significant cell death. The DNMT1-inhibitory activity of RRx-001 is clinically relevant in MM since: 1) DNMT1 is highly expressed in MM and correlates with disease progression[56]; 2) many tumor suppressor genes are hypermethylated in MM [4, 10, 11, 57, 58]; and importantly, a recent study showed that DNMT1-siRNA decreased viability and reactivates tumor suppressor genes *SOCS1* and *p16* in MM cells[45, 59].

The upstream mechanism(s) regulating DNMT1 are less well defined. USP7 inhibition increases ubiquitylation of DNMT1, and its degradation by the proteasome. We found that the combination of RRx-001 and USP7 inhibitor P5091 triggered synergistic anti-MM activity associated with a robust DNMT1 inhibition. While we observed activation of HDM2/p53 signaling in cells carrying wild-type p53, it may not be the mechanism explaining synergy noted in p53-null or mutant cells. As shown in our study, the anti-MM activity of RRx-001 can be attributed to induction of multiple apoptotic mechanisms, and is not completely dependent on p53. It is therefore likely that RRx-001-induced cell death in p53-null cells occurs via p53-independent pathways. One possibility is the activation of compensatory activity of p63 or p73 in p53 null ARP-1 or p53 mutant RPMI-8226 cells which can induce downstream p21; both p63 and p73 are regulated by ubiquitination process for stabilization and therefore may be target of USP7 or respond to P5091. In addition, the synergy between RRx-001 and USP7 inhibitor P5091 may be due to activation of other USP7 downstream targets besides p53. For example, prior studies have shown that knockdown of USP7 prevents rapid inactivation of the anti-proliferative transcription factor, FOXO4, providing a mechanism to impair the pro-survival PI3K/Akt pathway that is commonly activated in MM[60]. Therefore, USP7 inhibitor P5091 can simultaneously both activate pro-apoptotic via FOXO-mediated oxidative stress and inactivate pro-survival PI3K/Akt pathways. Thus, the synergy noted between RRx-001 and P5091 may be mediated by induction of pleiotropic apoptotic mechanisms and abrogation of survival pathways. Overall, these data provide the preclinical rationale for evaluating the combination of RRx-001 with USP7 inhibitor in future clinical trials.

As noted above, an additional mechanism of DNMT1 regulation is acetylation, exemplified by an earlier study showing that HDAC inhibitors degrades DNMT1 via acetylation. However, we did not observe DNMT1 acetylation in RRx-001-treated MM cells (data not shown). It is also possible that RRx-001-induced DNA damage activates an epigenetic mechanism requiring recruitment of DNMT1 on DNA and corresponding decrease in free soluble DNMT1 molecules, as seen in RRx-001-treated cells. These and other such mechanism(s) underlying the RRx-001-mediated decrease in DNMT1 remain to be defined.

In vitro studies showing RRx-001 activity were confirmed *in vivo* using the human MM.1S xenograft mouse model. Substantial reduction of tumor progression and enhancement of survival was observed in RRx-001-treated *versus* control mice. Our *in vivo* findings, coupled with our *in vitro* data showing minimal toxicity of RRx-001 against normal cells, confirmed that MM cells are more sensitive to epigenetic modulation than normal cells. Finally, we show that RRx-001 adds to anti-MM activity of bortezomib, pomalidomide, or HDAC inhibitor SAHA, confirming the potential clinical benefit of combining RRx-001 inhibitors with other agents.

Collectively, our preclinical studies demonstrate that DNMT1 plays a key role in MM cell survival versus DNMT3a or DNMT3b. Our findings show robust *in vitro* and *in vivo* anti-MM activity of RRx-001 is associated with downregulation of DNMTs as well as present the proof of concept for clinical studies of RRx-001, alone and in combination, to improve patient outcome in MM.

Supplementary Material

Refer to Web version on PubMed Central for supplementary material.

Acknowledgments

This investigation was supported by National Institutes of Health Specialized Programs of Research Excellence (SPORE) grant P50100707, PO1-CA078378, and RO1 CA050947. K.C.A. is an American Cancer Society Clinical Research Professor.

References

1. Anderson KC. Oncogenomics to target myeloma in the bone marrow microenvironment. Clinical cancer research : an official journal of the American Association for Cancer Research. 2011 Mar 15; 17(6):1225–1233. [PubMed: 21411438]
2. Dimopoulos M, Kyle R, Fermand JP, Rajkumar SV, San Miguel J, Chanan-Khan A, et al. Consensus recommendations for standard investigative workup: report of the International Myeloma Workshop Consensus Panel 3. Blood. 2011 May 5; 117(18):4701–4705. [PubMed: 21292778]
3. Colla S, Storti P, Donofrio G, Todoerti K, Bolzoni M, Lazzaretti M, et al. Low bone marrow oxygen tension and hypoxia-inducible factor-1alpha overexpression characterize patients with multiple myeloma: role on the transcriptional and proangiogenic profiles of CD138(+) cells. Leukemia. 2010 Nov; 24(11):1967–1970. [PubMed: 20811474]
4. Walker BA, Wardell CP, Chiecchio L, Smith EM, Boyd KD, Neri A, et al. Aberrant global methylation patterns affect the molecular pathogenesis and prognosis of multiple myeloma. Blood. 2011 Jan 13; 117(2):553–562. [PubMed: 20944071]
5. Azab AK, Hu J, Quang P, Azab F, Pitsillides C, Awwad R, et al. Hypoxia promotes dissemination of multiple myeloma through acquisition of epithelial to mesenchymal transition-like features. Blood. 2012 Jun 14; 119(24):5782–5794. [PubMed: 22394600]
6. Hu J, Van Valckenborgh E, Menu E, De Bruyne E, Vanderkerken K. Understanding the hypoxic niche of multiple myeloma: therapeutic implications and contributions of mouse models. Disease models & mechanisms. 2012 Nov; 5(6):763–771. [PubMed: 23115205]
7. Baylin SB. DNA methylation and gene silencing in cancer. Nature clinical practice Oncology. 2005 Dec; 2(Suppl 1):S4–S11.
8. Kondo Y. Epigenetic cross-talk between DNA methylation and histone modifications in human cancers. Yonsei medical journal. 2009 Aug 31; 50(4):455–463. [PubMed: 19718392]
9. Ng MH, Chung YF, Lo KW, Wickham NW, Lee JC, Huang DP. Frequent hypermethylation of p16 and p15 genes in multiple myeloma. Blood. 1997 Apr 1; 89(7):2500–2506. [PubMed: 9116295]

10. Dimopoulos K, Gimsing P, Gronbaek K. The role of epigenetics in the biology of multiple myeloma. Blood cancer journal. 2014; 4:e207. [PubMed: 24786391]
11. Heuck CJ, Mehta J, Bhagat T, Gundabolu K, Yu Y, Khan S, et al. Myeloma is characterized by stage-specific alterations in DNA methylation that occur early during myelomagenesis. Journal of immunology. 2013 Mar 15; 190(6):2966–2975.
12. Maes K, Menu E, Van Valckenborgh E, Van Riet I, Vanderkerken K, De Bruyne E. Epigenetic modulating agents as a new therapeutic approach in multiple myeloma. Cancers. 2013; 5(2):430–461. [PubMed: 24216985]
13. Chin HG, Esteve PO, Pradhan M, Benner J, Patnaik D, Carey MF, et al. Automethylation of G9a and its implication in wider substrate specificity and HP1 binding. Nucleic acids research. 2007; 35(21):7313–7323. [PubMed: 17962312]
14. de Carvalho F, Colleoni GW, Almeida MS, Carvalho AL, Vettore AL. TGFbetaR2 aberrant methylation is a potential prognostic marker and therapeutic target in multiple myeloma. International journal of cancer Journal international du cancer. 2009 Oct 15; 125(8):1985–1991. [PubMed: 19548309]
15. Tiedemann RL, Putiri EL, Lee JH, Hlady RA, Kashiwagi K, Ordog T, et al. Acute depletion redefines the division of labor among DNA methyltransferases in methylating the human genome. Cell reports. 2014 Nov 20; 9(4):1554–1566. [PubMed: 25453758]
16. Oronsky B, Oronsky N, Knox S, Fanger G, Scicinski J. Episensitization: therapeutic tumor resensitization by epigenetic agents: a review and reassessment. Anti-cancer agents in medicinal chemistry. 2014; 14(8):1121–1127. [PubMed: 24893730]
17. Ning S, Bednarski M, Oronsky B, Scicinski J, Saul G, Knox SJ. Dinitroazetidines are a novel class of anticancer agents and hypoxia-activated radiation sensitizers developed from highly energetic materials. Cancer research. 2012 May 15; 72(10):2600–2608. [PubMed: 22589277]
18. Oronsky B, Oronsky N, Scicinski J, Fanger G, Lybeck M, Reid T. Rewriting the epigenetic code for tumor resensitization: a review. Translational oncology. 2014 Oct; 7(5):626–631. [PubMed: 25389457]
19. Scicinski J, Oronsky B, Ning S, Knox S, Peehl D, Kim MM, et al. NO to cancer: The complex and multifaceted role of nitric oxide and the epigenetic nitric oxide donor, RRx-001. Redox biology. 2015 Jul 2.6:1–8. [PubMed: 26164533]
20. Reid T, Oronsky B, Scicinski J, Scribner CL, Knox SJ, Ning S, et al. Safety and activity of RRx-001 in patients with advanced cancer: a first-in-human, open-label, dose-escalation phase 1 study. The Lancet Oncology. 2015 Aug 18.
21. Chauhan D, Singh AV, Brahmandam M, Carrasco R, Bandi M, Hideshima T, et al. Functional interaction of plasmacytoid dendritic cells with multiple myeloma cells: a therapeutic target. Cancer cell. 2009 Oct 6; 16(4):309–323. [PubMed: 19800576]
22. Chauhan D, Tian Z, Nicholson B, Kumar KG, Zhou B, Carrasco R, et al. A small molecule inhibitor of ubiquitin-specific protease-7 induces apoptosis in multiple myeloma cells and overcomes bortezomib resistance. Cancer cell. 2012 Sep 11; 22(3):345–358. [PubMed: 22975377]
23. Das DS, Ray A, Song Y, Richardson P, Trikha M, Chauhan D, et al. Synergistic anti-myeloma activity of the proteasome inhibitor marizomib and the IMiD immunomodulatory drug pomalidomide. British journal of haematology. 2015 Oct 12.
24. Chauhan D, Singh A, Brahmandam M, Podar K, Hideshima T, Richardson P, et al. Combination of proteasome inhibitors bortezomib and NPI-0052 trigger in vivo synergistic cytotoxicity in multiple myeloma. Blood. 2008 Feb 1; 111(3):1654–1664. [PubMed: 18006697]
25. Chauhan D, Singh AV, Ciccarelli B, Richardson PG, Palladino MA, Anderson KC. Combination of novel proteasome inhibitor NPI-0052 and lenalidomide trigger in vitro and in vivo synergistic cytotoxicity in multiple myeloma. Blood. 2010 Jan 28; 115(4):834–845. [PubMed: 19965674]
26. Chou TC, Talalay P. Quantitative analysis of dose-effect relationships: the combined effects of multiple drugs or enzyme inhibitors. Advances in enzyme regulation. 1984; 22:27–55. [PubMed: 6382953]
27. Giuliani N, Storti P, Bolzoni M, Palma BD, Bonomini S. Angiogenesis and multiple myeloma. Cancer microenvironment : official journal of the International Cancer Microenvironment Society. 2011 Dec; 4(3):325–337. [PubMed: 21735169]

28. Podar K, Tai YT, Davies FE, Lentzsch S, Sattler M, Hideshima T, et al. Vascular endothelial growth factor triggers signaling cascades mediating multiple myeloma cell growth and migration. Blood. 2001; 98(2):428–435. [PubMed: 11435313]
29. Chauhan D, Uchiyama H, Akbarali Y, Urashima M, Yamamoto K, Libermann TA, et al. Multiple myeloma cell adhesion-induced interleukin-6 expression in bone marrow stromal cells involves activation of NF-kappa B. Blood. 1996 Feb 1; 87(3):1104–1112. [PubMed: 8562936]
30. Anderson KC. Targeted therapy of multiple myeloma based upon tumor-microenvironmental interactions. Experimental hematology. 2007 Apr; 35(4 Suppl 1):155–162.
31. Ray A, Tian Z, Das DS, Coffman RL, Richardson P, Chauhan D, et al. A novel TLR-9 agonist C792 inhibits plasmacytoid dendritic cell-induced myeloma cell growth and enhance cytotoxicity of bortezomib. Leukemia. 2014 Jan 30.
32. Ray A, Das DS, Song YPGR, Chauhan DKCA. Targeting PD1-PDL1 immune checkpoint in plasmacytoid dendritic cells interactions with T cells, natural killer cells, and multiple myeloma cells. Leukemia. 2015 *(In press)* 2015.
33. Lazebnik YA, Kaufmann SH, Desnoyers S, Poirier GG, Earnshaw WC. Cleavage of poly(ADP-ribose) polymerase by a proteinase with properties like ICE. Nature. 1994 Sep 22; 371(6495):346–347. [PubMed: 8090205]
34. Hockenbery DM, Oltvai ZN, Yin XM, Milliman CL, Korsmeyer SJ. Bcl-2 functions in an antioxidant pathway to prevent apoptosis. Cell. 1993 Oct 22; 75(2):241–251. [PubMed: 7503812]
35. Scicinski J, Oronsky B, Taylor M, Luo G, Musick T, Marini J, et al. Preclinical evaluation of the metabolism and disposition of RRx-001, a novel investigative anticancer agent. Drug metabolism and disposition: the biological fate of chemicals. 2012 Sep; 40(9):1810–1816. [PubMed: 22699395]
36. Scatena R, Bottoni P, Pontoglio A, Giardina B. Pharmacological modulation of nitric oxide release: new pharmacological perspectives, potential benefits and risks. Current medicinal chemistry. 2010; 17(1):61–73. [PubMed: 19941478]
37. Wang Z. Protein S-nitrosylation and cancer. Cancer letters. 2012 Jul 28; 320(2):123–129. [PubMed: 22425962]
38. Monteiro HP, Costa PE, Reis AK, Stern A. Nitric Oxide: Protein Tyrosine Phosphorylation and Protein S-Nitrosylation in Cancer. Biomedical journal. 2015 Jun 12.
39. Hess DT, Matsumoto A, Kim SO, Marshall HE, Stamler JS. Protein S-nitrosylation: purview and parameters. Nature reviews Molecular cell biology. 2005 Feb; 6(2):150–166. [PubMed: 15688001]
40. Hironaka K, Factor VM, Calvisi DF, Conner EA, Thorgeirsson SS. Dysregulation of DNA repair pathways in a transforming growth factor alpha/c-myc transgenic mouse model of accelerated hepatocarcinogenesis. Laboratory investigation; a journal of technical methods and pathology. 2003 May; 83(5):643–654. [PubMed: 12746474]
41. Kang MA, So EY, Simons AL, Spitz DR, Ouchi T. DNA damage induces reactive oxygen species generation through the H2AX-Nox1/Rac1 pathway. Cell death & disease. 2012; 3:e249. [PubMed: 22237206]
42. Burma S, Chen BP, Murphy M, Kurimasa A, Chen DJ. ATM phosphorylates histone H2AX in response to DNA double-strand breaks. The Journal of biological chemistry. 2001 Nov 9; 276(45): 42462–42467. [PubMed: 11571274]
43. Cottini F, Hideshima T, Suzuki R, Tai YT, Bianchini G, Richardson PG, et al. Synthetic Lethal Approaches Exploiting DNA Damage in Aggressive Myeloma. Cancer discovery. 2015 Sep; 5(9): 972–987. [PubMed: 26080835]
44. Lee BH, Yegnasubramanian S, Lin X, Nelson WG. Procainamide is a specific inhibitor of DNA methyltransferase 1. The Journal of biological chemistry. 2005 Dec 9; 280(49):40749–40756. [PubMed: 16230360]
45. Zhou W, Chen H, Hong X, Niu X, Lu Q. Knockdown of DNA methyltransferase-1 inhibits proliferation and derepresses tumor suppressor genes in myeloma cells. Oncology letters. 2014 Nov; 8(5):2130–2134. [PubMed: 25289094]
46. Kiziltepe T, Hideshima T, Catley L, Raje N, Yasui H, Shiraishi N, et al. 5-Azacytidine, a DNA methyltransferase inhibitor, induces ATR-mediated DNA double-strand break responses,

apoptosis, and synergistic cytotoxicity with doxorubicin and bortezomib against multiple myeloma cells. Molecular cancer therapeutics. 2007 Jun; 6(6):1718–1727. [PubMed: 17575103]

47. Szklarczyk D, Franceschini A, Wyder S, Forslund K, Heller D, Huerta-Cepas J, et al. STRING v10: protein-protein interaction networks, integrated over the tree of life. Nucleic acids research. 2015 Jan; 43(Database issue):D447–D452. [PubMed: 25352553]
48. Felle M, Joppien S, Nemeth A, Diermeier S, Thalhammer V, Dobner T, et al. The USP7/Dnmt1 complex stimulates the DNA methylation activity of Dnmt1 and regulates the stability of UHRF1. Nucleic acids research. 2011 Oct; 39(19):8355–8365. [PubMed: 21745816]
49. Bergsagel PL, Kuehl WM. Molecular pathogenesis and a consequent classification of multiple myeloma. Journal of clinical oncology : official journal of the American Society of Clinical Oncology. 2005 Sep 10; 23(26):6333–6338. [PubMed: 16155016]
50. Bergsagel PL, Chesi M, Nardini E, Brents LA, Kirby SL, Kuehl WM. Promiscuous translocations into immunoglobulin heavy chain switch regions in multiple myeloma. Proceedings of the National Academy of Sciences of the United States of America. 1996 Nov 26; 93(24):13931–13936. [PubMed: 8943038]
51. Du Z, Song J, Wang Y, Zhao Y, Guda K, Yang S, et al. DNMT1 stability is regulated by proteins coordinating deubiquitination and acetylation-driven ubiquitination. Science signaling. 2010; 3(146) ra80.
52. Kuhn D, Bjorklund C, Magarotto V, Mathews J, Wang M, Baladandayuthapani V, et al. Bortezomib resistance is mediated by increased signaling through the insulin-like growth factor-1/Akt axis. ASH Annual Meeting Abstracts. 2009; 114(22):2739.
53. Magesh S, Chen Y, Hu L. Small molecule modulators of Keap1-Nrf2-ARE pathway as potential preventive and therapeutic agents. Medicinal research reviews. 2012 Jul; 32(4):687–726. [PubMed: 22549716]
54. Ning S, Sekar TV, Scicinski J, Oronsky B, Peehl DM, Knox SJ, et al. Nrf2 activity as a potential biomarker for the pan-epigenetic anticancer agent, RRx-001. Oncotarget. 2015 Jun 4.
55. Afanas'ev I. New nucleophilic mechanisms of ros-dependent epigenetic modifications: comparison of aging and cancer. Aging and disease. 2014 Feb; 5(1):52–62. [PubMed: 24490117]
56. Bollati V, Fabris S, Pegoraro V, Ronchetti D, Mosca L, Deliliers GL, et al. Differential repetitive DNA methylation in multiple myeloma molecular subgroups. Carcinogenesis. 2009 Aug; 30(8): 1330–1335. [PubMed: 19531770]
57. Kaiser MF, Johnson DC, Wu P, Walker BA, Brioli A, Mirabella F, et al. Global methylation analysis identifies prognostically important epigenetically inactivated tumor suppressor genes in multiple myeloma. Blood. 2013 Jul 11; 122(2):219–226. [PubMed: 23699600]
58. Walton EL, Francastel C, Velasco G. Maintenance of DNA methylation: Dnmt3b joins the dance. Epigenetics. 2011 Nov; 6(11):1373–1377. [PubMed: 22048250]
59. Wang X, Zhang L, Ding N, Yang X, Zhang J, He J, et al. Identification and characterization of DNAzymes targeting DNA methyltransferase I for suppressing bladder cancer proliferation. Biochemical and biophysical research communications. 2015 May 29; 461(2):329–333. [PubMed: 25888794]
60. van der Horst A, de Vries-Smits AM, Brenkman AB, van Triest MH, van den Broek N, Colland F, et al. FOXO4 transcriptional activity is regulated by monoubiquitination and USP7/HAUSP. Nature cell biology. 2006 Oct; 8(10):1064–1073. [PubMed: 16964248]

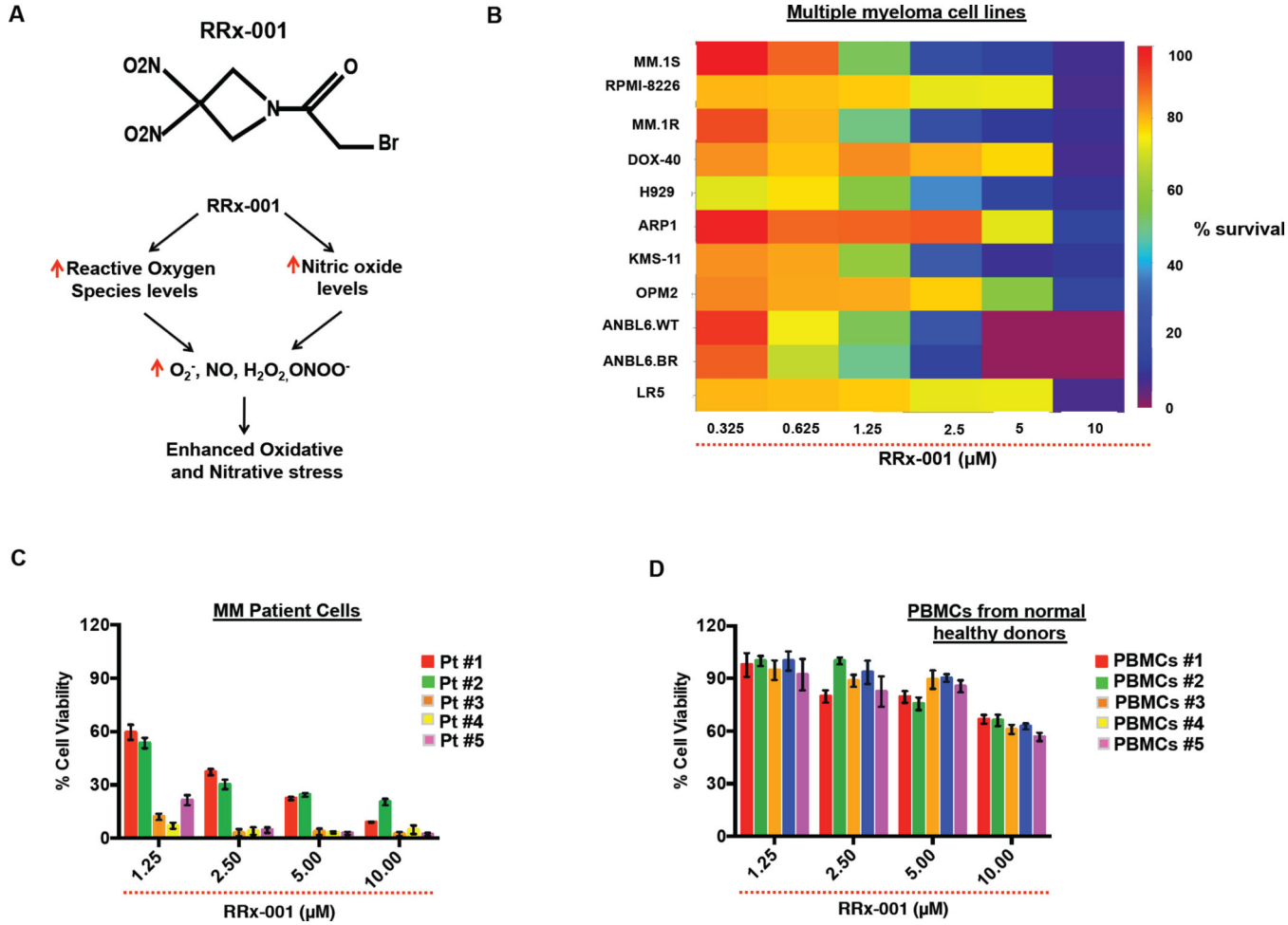

Figure 1. Anti-MM activity of RRx-001

(A) Chemical structure of RRx-001. Schema: RRx-001-induces Reactive Oxygen and Nitrogen Species (RONS), which in turn induce oxidative and nitrative stress causing cell death. (B) MM-cell lines (MM.1S, RPMI-8226, MM.1R, DOX-40, H929, ARP1, KMS-11, OPM2, LR5, ANBL6.WT and ANBL6.BR) were treated with DMSO or RRx-001 for 24h, followed by assessment for cell viability using WST-1 assay (mean ± SE; $p < 0.05$ for all cell lines; n=3). Cell viability data is presented in a Heatmap. (C) Purified patient MM cells (CD138-positive) were treated with DMSO or RRx-001 for 24h, followed by assessment for cell viability using CellTiter-Glo assay (mean ± SE of triplicate cultures; $p < 0.001$ for all patient samples PT#1-Pt#5). (D) Normal PBMCs from healthy Donors (PBMCs#1-PBMCs#5) were treated with indicated concentrations of RRx-001 for 24h, and then analyzed for viability using WST-1 assay (mean ± SE of quadruplicate cultures).

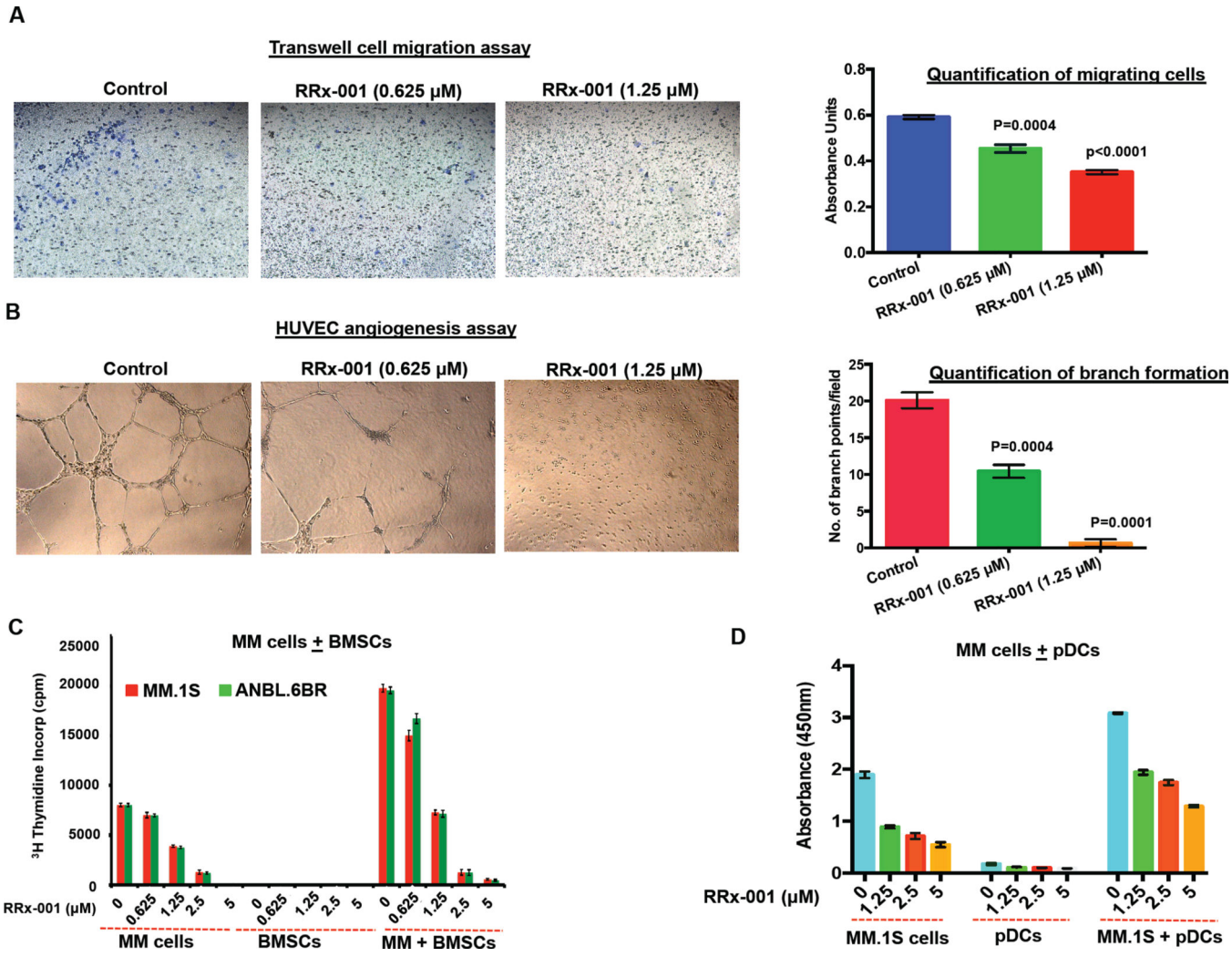

Figure 2. RRx-001 blocks migration, tubule formation, and cytoprotective effects of BMSCs and pDCs

(A) Migration assay: MM.1S cells were treated with DMSO or RRx-001 for 12h; cells were >90% viable at this time point. The cells were then washed and cultured in serum-free medium. After 2h incubation, cells were plated on a fibronectin-coated polycarbonate membrane in the upper chamber of transwell inserts and exposed for 4h to serum-containing medium in the lower chamber. Cells migrating to the bottom face of the membrane were fixed with 90% ethanol and stained with crystal violet. A total of 3 randomly selected fields were examined for cells that had migrated from top to bottom chambers. (Left panel) Image is representative of 2 experiments with similar results. (Right panel) The bar graph represents quantification of migrated cells. Data are mean ± SE ($p < 0.001$). (B) HUVECs were cultured in the presence or absence of RRx-001 for 12h, and then assessed for *in vitro* angiogenesis using matrigel capillary-like tube structure formation assays (Left panel). Image is representative from 3 experiments with similar results. *In vitro* angiogenesis is reflected by capillary tube branch formation (dark brown). (Right panel) The bar graph represents quantification of capillary-like tube structure formation in response to indicated agents: Branch points in several random view fields/well were counted, values were

averaged, and statistically significant differences were measured using Student's *t* test. (C) MM.1S cells were cultured with or without BMSCs for 24h in the presence or absence of RRx-001, and DNA synthesis was measured by ^{3}H-TdR uptake (mean ± SD of triplicate cultures; $p < 0.001$ for all samples). (D) MM.1S cells were cultured with or without pDCs for 24h in the presence or absence of RRx-001, and cell growth was assessed using WST1 assay (mean ± SE of triplicate cultures; $p < 0.001$ for all samples).

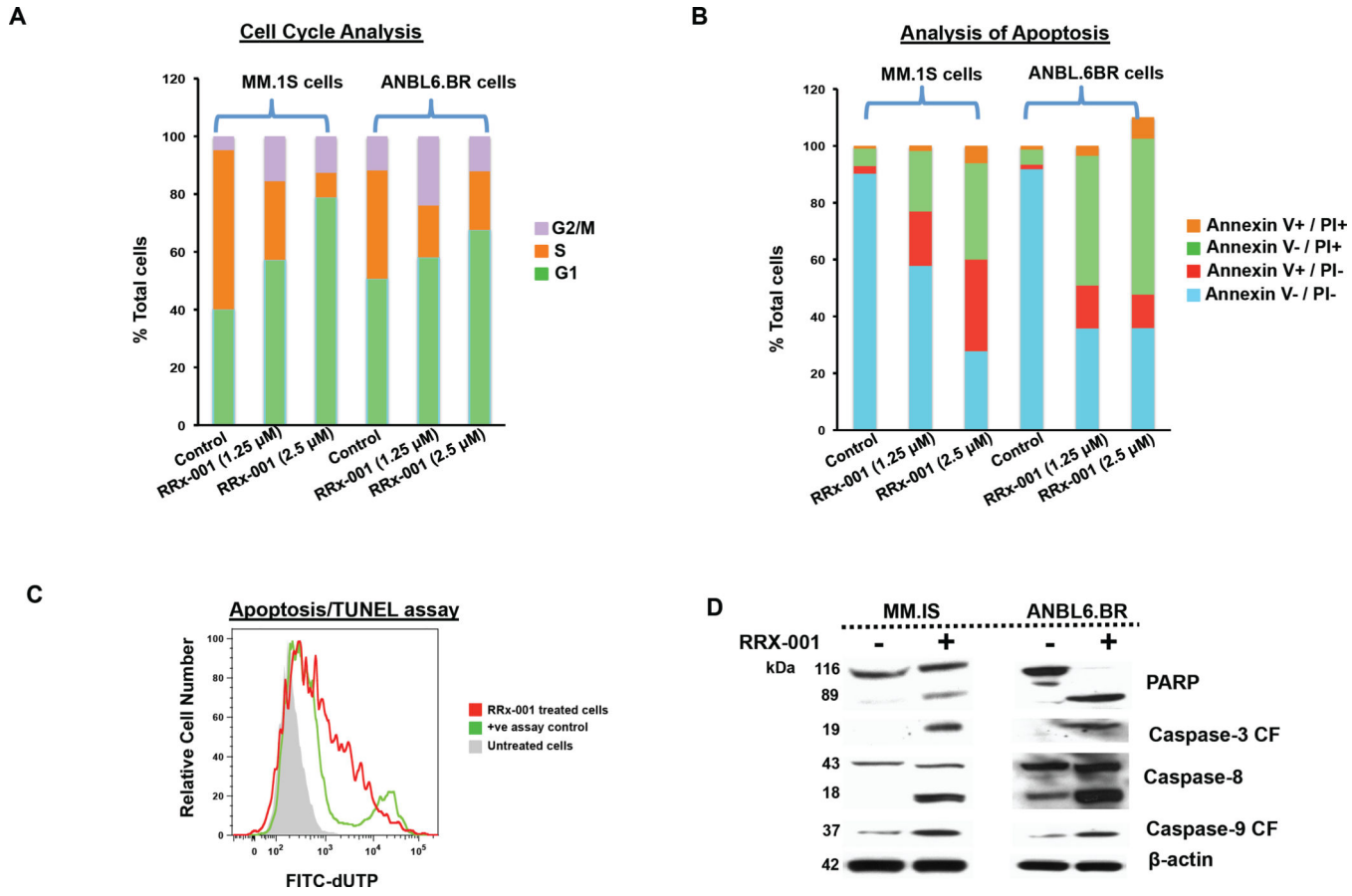

Figure 3. RRx-001 induces growth arrest and apoptosis in MM cells

(A) MM.1S and ANBL.6BR cells were treated with indicated concentrations of RRx-001 for 12h, and fixed in 70% ethanol. After washing with phosphate-buffered saline, cells were stained with propidium idodide (PI), and DNA content of cells was analyzed using fluorescence-activated cell sorter. Bar graph shows percentage of cell populations in G2/M-, S-, or G1-phase of cell cycle. (B) MM.1S and ANBL.6BR cells were treated with RRx-001 for 18h, and then analyzed for apoptosis using Annexin V/PI staining assay. (C) MM.1S cells were treated with RRx-001 (1.25 μM) for 18h, followed by end-labeling with FITC-conjugated dUTP and analysis/quantification of TUNEL positive cells by FACS. (D) MM.1S and ANBL.6BR cells were treated with RRx-001 (1.25 μM) for 12h; protein lysates were subjected to immunoblot analysis using antibodies (Abs) specific against PARP, caspase-3, caspase-8, caspase-9 or β-actin. CF, cleaved fragment. Blots shown are representative of 3 independent experiments.

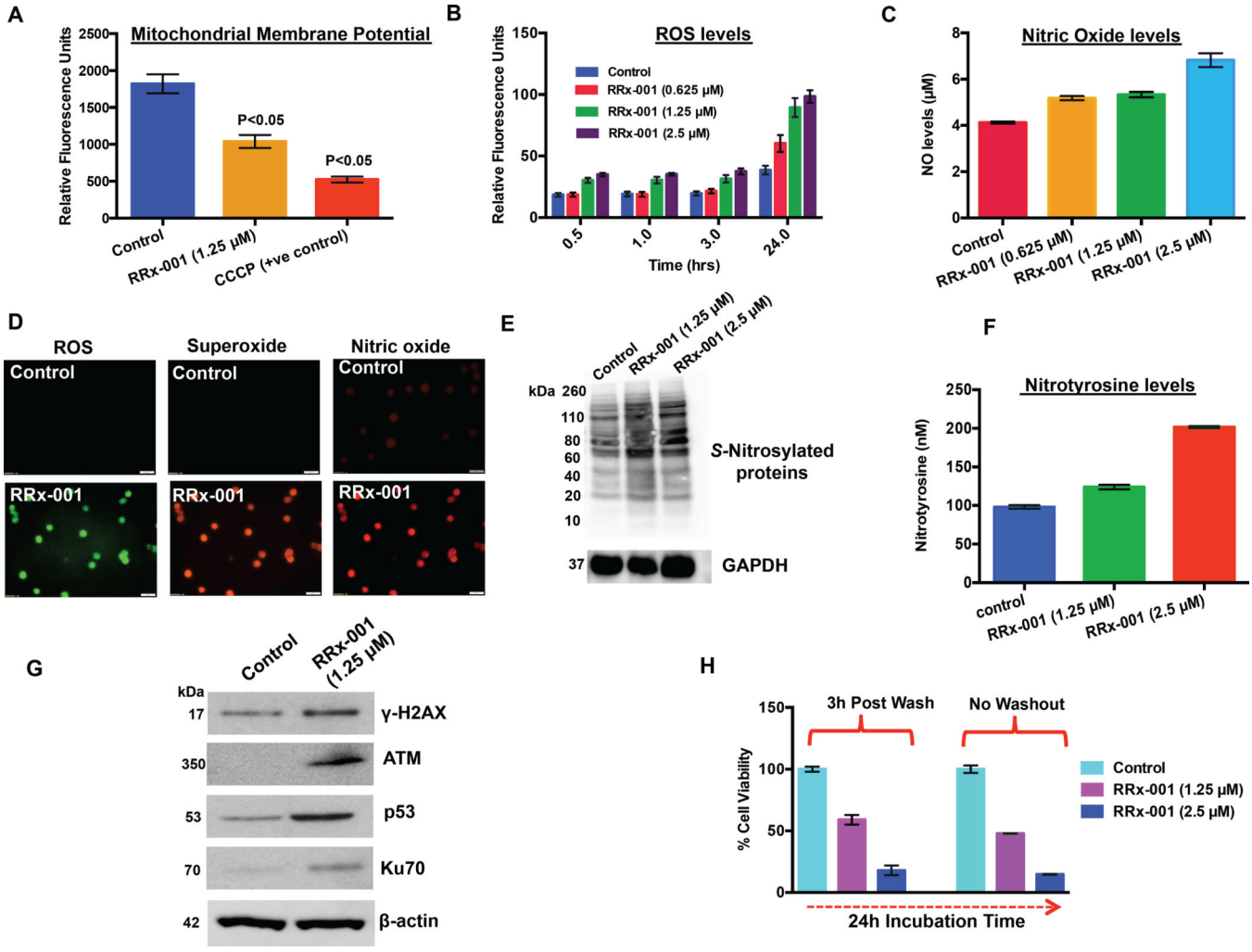

Figure 4. Mechanisms mediating anti-MM activity of RRx-001

(A) MM.1S cells were pretreated with DMSO control, or RRx-001 (1.25 μM) for 6h; cells were then stained with fluorescent cationic dye JC-1 (MitoPT™) for 20 mins, followed by analysis of mitochondrial membrane potential (ΔΨm) using fluorescence emission intensity (mean ± SE; $p < 0.005$, $n = 3$). Cells were also treated with CCCP (Carbonyl cyanide *m*-chlorophenyl hydrazine) as a positive control for alteration in ΔΨm triggered by inhibition of oxidative phosphorylation. (B) MM.1S cells were labeled with cell permeable 2',7' –dichlorofluorescein diacetate (DCFDA) (20 μM) fluorogenic dye that measures cellular reactive oxygen species; cell were then treated with DMSO control or RRx-001 for 6h, followed by analysis of 2',7' –dichlorofluorescein (DCF) fluorescent compound levels using fluorescence emission intensity (mean ± SE; $p < 0.001$, $n = 3$) (C) MM.1S cells were treated with DMSO control or RRx-001 for 6h; cells were harvested and cytosolic extracts were then analyzed for nitric oxide (NO) levels using colorimetric assay kit (mean ± SE; $p < 0.005$, $n = 3$). (D) Analysis of real time reactive oxygen and nitrogen species (RONS) in live cells using fluorescence microscopy: MM.1S cells were seeded onto glass slides and incubated with ROS/RNS 3-Plex detection reagent for 2h; cells were washed and then treated with DMSO control or RRx-001 (1.25 μM) for 2h, followed by analysis using

fluorescence/confocal microscopy. ROS, NO, and superoxide were detected using filter sets compatible with fluorescein Excitation/Emmission: 490/525nm, 550/620nm, and 650/670nm, respectively. Images were obtained with a Leica SP5X laser scanning confocal microscope (100x magnification). (E) MM.1S cells were treated with DMSCO control or RRx-001 for 12h; cytosolic protein extracts were then subjected to immunoblot analysis using antibodies specific against *S*-Nitrosylated proteins and GAPDH. Blots shown are representative of three independent experiments with similar results. (F) MM.1S cells were treated DMSO control or RRx-001 for 12h; total cell lysate were then incubated with tetranitromethane (TNM) for nitration, followed by analysis of 3-nitrotyrosine levels using OxiSelect Nitrotyrosine ELISA kit (mean ± SE; $p < 0.005$; $n = 3$). (G) MM.1S cells were treated with DMSO control or RRx-001 for 12h; protein lysates were then subjected to immunoblot analysis using antibodies specific against γ-H2AX, ATM, p53, Ku70, or β-actin. Blots shown are representative of three independent experiments with similar results. (H) MM.1S cells were treated with DMSO control or RRx-001 for 3h; cells were washed to remove drugs and then cultured in fresh complete medium for 24h, followed by analysis of viability using WST-1 assay (mean ± SE; $p < 0.005$, $n=3$). In addition, cells were treated with RRx-001 continuously for 24h, and then subjected to analysis viability (mean ± SD; $p < 0.005$, $n=3$).

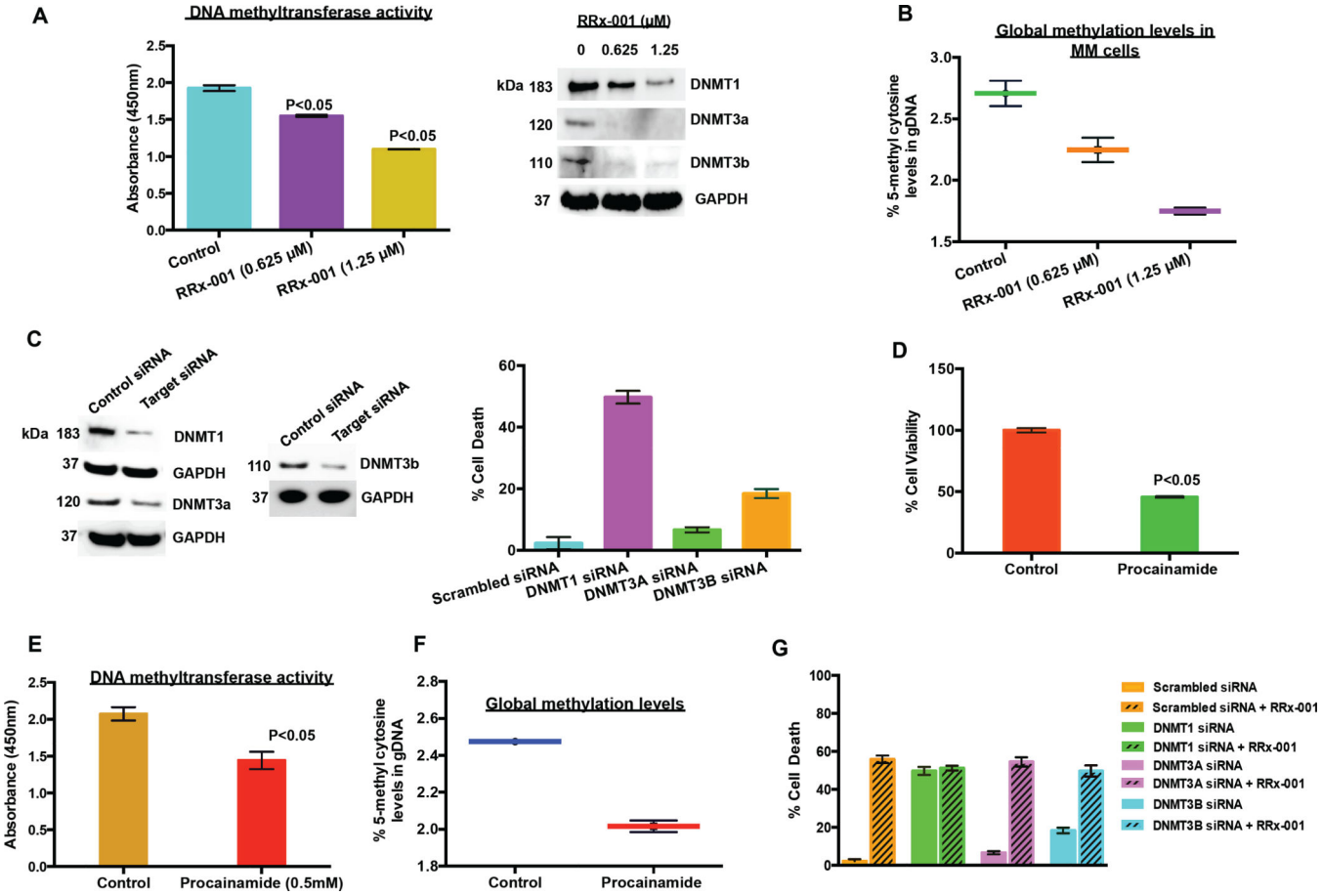

Figure 5. RRx-001 inhibits DNA methyltransferases activity and global methylation in MM cells

(A) Bar Graph: MM.1S cells were treated with DMSO control or RRx-001 for 12h; protein extracts were analyzed for total DNMT activity using EpiQuik DNMT activity kit. Immunoblot: MM.1S cells were treated with DMSO control or RRx-001 for 12h; protein lysates were subjected to immunoblot analysis using antibodies specific against with DNMT1, DNMT3A, DNMT3B, or GAPDH. (B) Assessment of global methylation: MM.1S cells were treated with DMSO control or RRx-001 for 12h; cells were harvested and then genomic DNA was purified, followed by quantification of 5-methyl cytosine in each sample using MethylFlash methylated DNA Quantification Kit (mean ± SD; $p < 0.005$; n=3). (C) Immunoblot: MM.1S cells were transfected with genome control-siRNA/scr-siRNA, DNMT1-siRNA, DNMT3A-siRNA, or DNMT3B–siRNA; cells were harvested 24h post-transfection, and protein lysates were subjected to immunoblot analysis using antibodies specific against DNMT1, DNMT3A, DNMT3B, or GAPDH. Bar Graph: MM.1S cells were transfected with genome control-siRNA/scr-siRNA, DNMT1-siRNA, DNMT3A-siRNA, or DNMT3B–siRNA and cultured in complete medium for 72h, followed by analysis of cell death (mean ± SE; $p < 0.005$, n=3). (D) MM.1S cells were treated with DMSO control or procainamide (0.5mM) for 24h, followed by analysis for cell viability using WST-1 assay (mean ± SD; $p < 0.001$, n=3). (E) MM.1S cells were treated with DMSO control or procainamide (0.5μM) for 24h; protein extracts were analyzed for total DNMT activity using EpiQuik DNMT activity kit (mean ± SE; $p < 0.05$; n=3). (F) MM.1S cells were treated with

DMSO control or RRx-001 for 24h; cells were harvested and then genomic DNA was purified, followed by analysis of global methylation by quantification of 5-methyl cytosine in each sample using MethylFlash methylated DNA Quantification Kit (mean ± SD; $p < 0.005$; n=3). (G) MM.1S cells were transfected with scr-siRNA, DNMT1-siRNA, DNMT3A-siRNA, or DNMT3B–siRNA and cultured in complete medium for 24h; cells were then treated with DMSO or RRx-001 for 24h, followed by analysis of cell death (mean ± SD; $p < 0.001$, n=3).

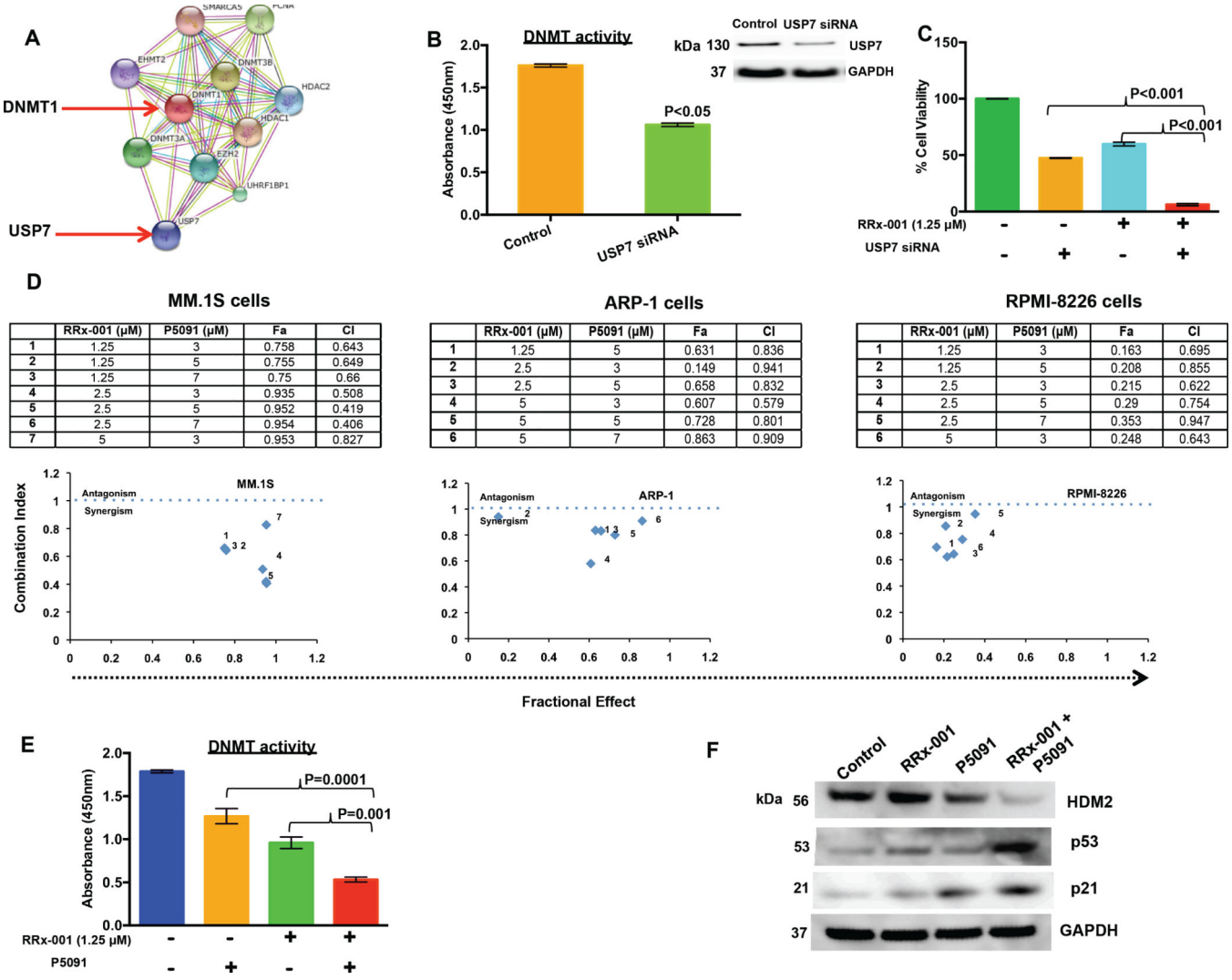

	RRx-001 (μM)	P5091 (μM)	Fa	CI
1	1.25	3	0.758	0.643
2	1.25	5	0.755	0.649
3	1.25	7	0.75	0.66
4	2.5	3	0.935	0.508
5	2.5	5	0.952	0.419
6	2.5	7	0.954	0.406
7	5	3	0.953	0.827

	RRx-001 (μM)	P5091 (μM)	Fa	CI
1	1.25	5	0.631	0.836
2	2.5	3	0.149	0.941
3	2.5	5	0.658	0.832
4	5	3	0.607	0.579
5	5	5	0.728	0.801
6	5	7	0.863	0.909

	RRx-001 (μM)	P5091 (μM)	Fa	CI
1	1.25	3	0.163	0.695
2	1.25	5	0.208	0.855
3	2.5	3	0.215	0.622
4	2.5	5	0.29	0.754
5	2.5	7	0.353	0.947
6	5	3	0.248	0.643

Figure 6. Blockade of deubiquitylated enzyme USP7 enhances anti-MM activity of RRx-001

(A) Analysis of DNMT1 interacting proteins using STRING protein ineraction database (Network mapping) (B) MM.1S cells were transfected with scr-siRNA or USP7 siRNA and cultured in complete medium for 24h; protein extracts were then analyzed for total DNMT activity using EpiQuik DNMT activity kit (mean ± SD; $p < 0.001$; n=3). Immunoblot shows USP7 expression in cells transfected with scr-siRNA or USP7-siRNA. (C) MM.1S cells were transfected with scr-siRNA or USP7 siRNA; cells were then treated with DMSO control or RRx-001 (1.25 μM) for 24h, followed by analysis for cell viability (mean ± SD; $p < 0.005$ for control versus RRx-001-treated samples; n=3). (D) MM.1S, ARP-1, and RPMI-8226 were treated with RRx-001, P5091, or RRx-001 plus P5091 for 24h; and then assessed for cell viability using WST1 assay. Isobologram analysis shows the synergistic anti-MM activity of RRx-001 and P5091. The graph (lower panels) is derived from the values given in the table (upper panels). Combination index (CI) <1 indicates synergy. (E) MM.1S cells were treated with RRx-001 (1.25μM), P5091 (3μM), or RRx-001 plus P5091 for 12h; protein extracts were analyzed for total DNMT activity using EpiQuik DNMT activity kit (mean ± SD; $p < 0.001$; n=3). (F) MM.1S cells were treated with RRx-001 (1.25

μM), P5091 (3 μM), or RRx-001 plus P5091 for 12h; protein lysates were then subjected to immunoblot analysis using antibodies specific against p21, HDM2, p53, or GAPDH.

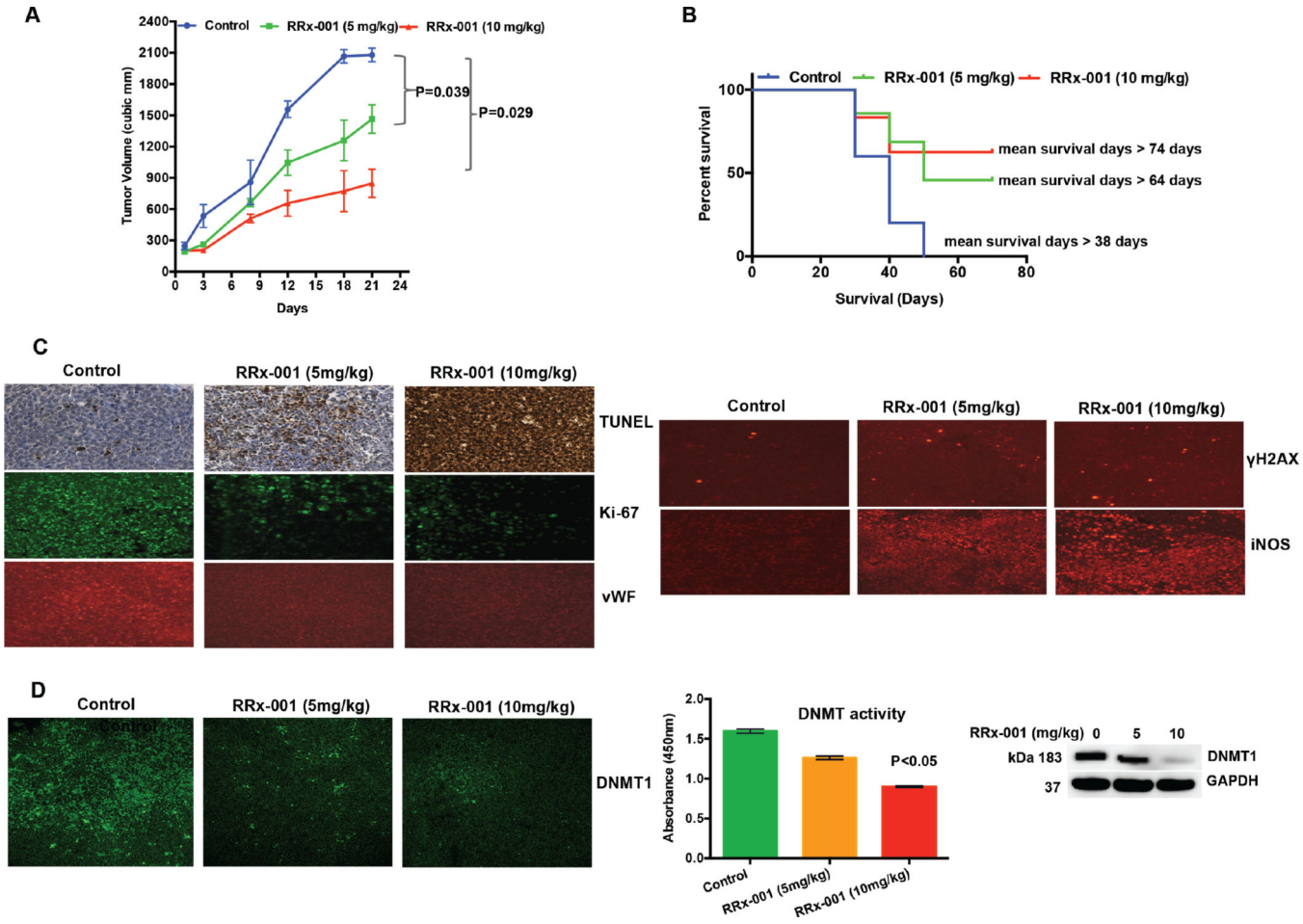

Figure 7. RRx-001 inhibits human plasmacytoma growth and prolongs survival in CB-17 SCID mice as well as targets DNMT1 *in vivo*

(A) Mice bearing human MM.1S MM tumors were treated with either vehicle control, or RRx-001 (5 mg/kg; 10 mg/kg; i.v.) three times weekly for 21 days. Average and standard deviation of tumor volume (mm^3) is shown versus time when tumor was measured (mean tumor volume ± SD, 5 mice/group). (B) Kaplan-Meier plots shows survival in mice. RRx-001-treated mice show significantly increased survival versus vehicle control-treated mice ($p < 0.05$; student's t-test). (C) Tumor sections from vehicle control- and RRx-001-treated mice were subjected to immunostaining using TUNEL, anti-Ki67, anti-vWF, anti-γ-H2AX, or anti-iNOS Abs. All Images were obtained with a Leica SP5X laser scanning confocal microscope (40x magnification). Micrographs shown are representative of similar observations in 2 mice receiving the same treatment (D) Micrograph: Tumors harvested from mice were immunostained with anti-DNMT1 Ab. Bar graph: Protein extracts from harvested tumors were analyzed for total DNMT activity using EpiQuik DNMT activity kit (mean ± SD; $p < 0.005$ n=3). Immunoblot: Tumor lysates from control- and RRx-001-treated mice were subjected to immunoblot analysis using anti-DNMT1 or anti-GAPDH Abs.